Arthritis & Rheumatology
Vol. 71, No. 4, April 2019, pp 571–582
DOI 10.1002/art.40765

AMERICAN COLLEGE OF RHEUMATOLOGY
EDUCATION • TREATMENT • RESEARCH

Targeted Inhibition of Aggrecanases Prevents Articular Cartilage Degradation and Augments Bone Mass in the STR/Ort Mouse Model of Spontaneous Osteoarthritis

Ioannis Kanakis,[1] Ke Liu,[1] Blandine Poulet,[1] Behzad Javaheri,[2] Rob J. van 't Hof,[1] Andrew A. Pitsillides,[2] and George Bou-Gharios[1]

Objective. Cartilage destruction in osteoarthritis (OA) is mediated mainly by matrix metalloproteinases (MMPs) and ADAMTS. The therapeutic candidature of targeting aggrecanases has not yet been defined in joints in which spontaneous OA arises from genetic susceptibility, as in the case of the STR/Ort mouse, without a traumatic or load-induced etiology. In addition, we do not know the long-term effect of aggrecanase inhibition on bone. We undertook this study to assess the potential aggrecanase selectivity of a variant of tissue inhibitor of metalloproteinases 3 (TIMP-3), called [-1A]TIMP-3, on spontaneous OA development and bone formation in STR/Ort mice.

Methods. Using the background of STR/Ort mice, which develop spontaneous OA, we generated transgenic mice that overexpress [-1A]TIMP-3, either ubiquitously or conditionally in chondrocytes. [-1A]TIMP-3 has an extra alanine at the N-terminus that selectively inhibits ADAMTS but not MMPs. We analyzed a range of OA-related measures in all mice at age 40 weeks.

Results. Mice expressing high levels of [-1A]TIMP-3 were protected against development of OA, while those expressing low levels were not. Interestingly, we also found that high levels of [-1A]TIMP-3 transgene overexpression resulted in increased bone mass, particularly in females. This regulation of bone mass was at least partly direct, as adult mouse primary osteoblasts infected with [-1A]TIMP-3 in vitro showed elevated rates of mineralization.

Conclusion. The results provide evidence that [-1A]TIMP-3–mediated inhibition of aggrecanases can protect against cartilage degradation in a naturally occurring mouse model of OA, and they highlight a novel role that aggrecanase inhibition may play in increased bone mass.

INTRODUCTION

Osteoarthritis (OA) is characterized by altered homeostasis of articular cartilage and abnormal bone formation. OA development depends on a balance of extracellular matrix (ECM) production and degradation. Proteolytic enzymes such as ADAMTS as well as matrix metalloproteinases (MMPs) are found to be up-regulated in OA joints (1–5) and are directly involved in OA pathophysiology (6,7). Therefore, inhibition of these metalloproteinases is a potential route for the design of pharmaceutical agents to retard, suppress, and even halt the progression of OA. However, broad-spectrum inhibitors of MMPs, which were shown to be chondroprotective in animal models, raised safety concerns in a clinical trial, pinpointing a need for inhibitors with greater specificity (8). In C57BL/6 mice, loss of activity of key catabolic enzymes, such as ADAMTS-5, protects against OA lesions (9–11) compared with deletion of ADAMTS-1 or ADAMTS-4, which suggests that ADAMTS-5 plays a central role in mouse models of inflammatory- and surgically induced OA (12,13). However, more recent data suggest that another aggrecanase, not yet determined, cleaves aggrecan before its secretion. Moreover, a noncatalytic function of ADAMTS-5 is suggested to have competitive interactions with major endocytic recycling machinery (14).

Investigators using STR/Ort mice as a model of human OA have proved that genetic susceptibility is a solid basis for assessing the protection afforded by novel treatment (15,16). Crucially, OA in STR/Ort mice closely resembles human OA and progresses to cartilage loss, along with similar alterations in bone mass and structure (17–20). Pertinently, it has been shown that the OA-related proteoglycan depletion observed predominantly across

Supported by Versus Arthritis (grants 20039 and 20581).

[1]Ioannis Kanakis, PhD, Ke Liu, PhD, Blandine Poulet, PhD, Rob J. van 't Hof, PhD, George Bou-Gharios, PhD: University of Liverpool, Liverpool, UK; [2]Behzad Javaheri, PhD, Andrew A. Pitsillides, PhD: Royal Veterinary College, London, UK.

No potential conflicts of interest relevant to this article were reported.

Address correspondence to George Bou-Gharios, PhD, Institute of Ageing and Chronic Disease, Faculty of Health & Life Sciences, William Henry Duncan Building, 6 West Derby Street, L7 8TX Liverpool, UK. E-mail: ggharios@liverpool.ac.uk.

Submitted for publication April 10, 2018; accepted in revised form October 25, 2018.

the medial tibial compartment in STR/Ort mouse joints also likely involves both collagenase and aggrecanase activities, as in humans (20,21). Interestingly, compared with C57BL/6 mice, female STR/Ort mice have high bone mass, with bone marrow compression and extramedullary hematopoiesis observed by age 36 weeks (22). Consistently, recent studies from our group showed that this difference is present even in young STR/Ort mice, which have increased cortical and trabecular parameters compared with age-matched CBA mice (23). These characteristics make the STR/Ort strain an intriguing and hitherto unexplored target in which to explore potentially protective transgenic strategies.

Tissue inhibitor of metalloproteinases 3 (TIMP-3) is a native biologic inhibitor of enzyme activity for members of the metzincin family, including collagenases (MMPs 1, 8, and 13), gelatinases (MMPs 2 and 9), and aggrecanases (ADAMTS-4 and ADAMTS-5). Extracellular trafficking of TIMP-3 is regulated by the competition between ECM binding and endocytosis via low-density lipoprotein receptor–related protein 1 (LRP-1) (24–26). It has previously been shown that modifications in TIMP-3 expression could modify joint degeneration (27) and that loss/gain of TIMP-3 function leads to significant alteration in bone structure (28,29). In the present study, we have used a variant of TIMP-3, named [-1A]TIMP-3, which harbors a single alanine addition to the amino-terminal end, which was shown to inhibit aggrecanases, namely ADAMTS-4/5, with much greater selectivity than other MMPs (30,31). This modified activity is driven by conformational changes, in which the active site is tilted and the interaction of Phe^{34} of the inhibitor with MMPs is lost (31).

Our aim was to assess the potential aggrecanase selectivity of [-1A]TIMP-3 on spontaneous OA development and bone formation in STR/Ort mice. We found that high levels of [-1A]TIMP-3 expression in transgenic STR/Ort mice can effectively attenuate cartilage destruction and OA-related subchondral thickening, but, strikingly, can also significantly augment bone mass.

MATERIALS AND METHODS

Generation of lentiviral and plasmid vectors to overexpress [-1A]TIMP-3. The lentivirus vector was constructed by cloning [-1A]TIMP-3 with a FLAG tag into the *Eco* RV–*Sal* I site of the pCCL-expressing vector driven by the elongation factor 1α (EF-1α) promoter. The construct also contained nerve growth factor receptor (NGFR) as a marker (Figure 1A).

We cotransfected 293T17 cells with transfer vector and packaging vectors by electroporation using a Neon transfection system (Invitrogen) to produce the virus. Viral supernatants were harvested 48 and 72 hours after transfection and concentrated by ultracentrifugation at 10,000*g* for 2 hours. The viral pellet was collected and dissolved in phosphate buffered saline (PBS).

A second conditional plasmid was generated using the Col2a1 3-kb promoter and the 3-kb first intron that drives specific expression in chondrocytes (32). The [-1A]TIMP-3 complementary DNA (cDNA) was followed by an internal ribosome entry site and a β-galactosidase reporter gene (Figure 1B).

Transient transduction was performed at 10 multiplicities of infection in 2 cell lines, HEK 293 and HTB94, to test integration efficacy and overexpression capacity. Flow cytometry with allophycocyanin-conjugated anti-NGFR was used to estimate transfection efficiency. Trichloroacetic acid (TCA) protein precipitation and Western blotting were used to test [-1A]TIMP-3 protein levels.

Animals. An STR/Ort mouse colony maintained at Royal Veterinary College, London was used to generate transgenic mice overexpressing [-1A]TIMP-3 on this background. Each fertilized embryo was injected with either Col2a1[-1A]TIMP-3 linearized plasmid in male pro nucleus or by infection using 100 lentiviral particles (EF-1α[-1A]TIMP-3) per embryo. The latter procedure was also used to generate transgenic mice in the control CBA strain (EF-1α[-1A]TIMP-3–transgenic CBA mice). Newborn transgenic mice were routinely genotyped by quantitative polymerase chain reaction (qPCR) using the reporter gene LacZ as well as the [-1A]TIMP-3 insert (see Supplementary Table 1, available on the *Arthritis & Rheumatology* web site at http://onlinelibrary.wiley.com/doi/10.1002/art.40765/abstract). All experimental protocols were performed in compliance with the UK Animals (Scientific Procedures) Act 1986 regulations.

We analyzed hind limb bones and knee joints isolated from STR/Ort mice at age 40 weeks. Age-matched nontransgenic (untreated) STR/Ort mice or transgenic CBA mice, a parental background strain of STR/Ort mice, were used as controls. The exact number of animals used in each analysis is described in Supplementary Table 2, http://onlinelibrary.wiley.com/doi/10.1002/art.40765/abstract.

Western blotting. Cultured media from transfected HEK 293 and HTB94 cells were precipitated with TCA, resuspended in PBS to equal total protein content, resolved by 10% sodium dodecyl sulfate–polyacrylamide gel electrophoresis under reducing conditions, and electrotransferred to Hybond P PVDF membranes (Amersham Biosciences). Membranes were blocked with 5% skim milk and probed overnight at 4°C with rabbit polyclonal anti–TIMP-3 antibody (1:2,000 dilution, AB6000; Millipore), followed by incubation with horseradish peroxidase (HRP)–labeled goat anti-rabbit antibody (1:10,000 dilution; Dako). Analysis was performed using an ECL Advanced Western Blotting Detection Kit (Amersham Biosciences). For Western blots using mouse tails, 250 mg of tissue was boiled at 95°C for 10 minutes in Laemmli buffer, and samples were electrophoresed in 4–12% Bis-Tris precast gels (NuPAGE) at 200V for 35 minutes. Proteins were transferred on PVDF membranes, blocked, and incubated overnight with either anti–TIMP-3 antibody or rabbit anti–β-actin (ab8227; Abcam). Detection was performed using fluorescent

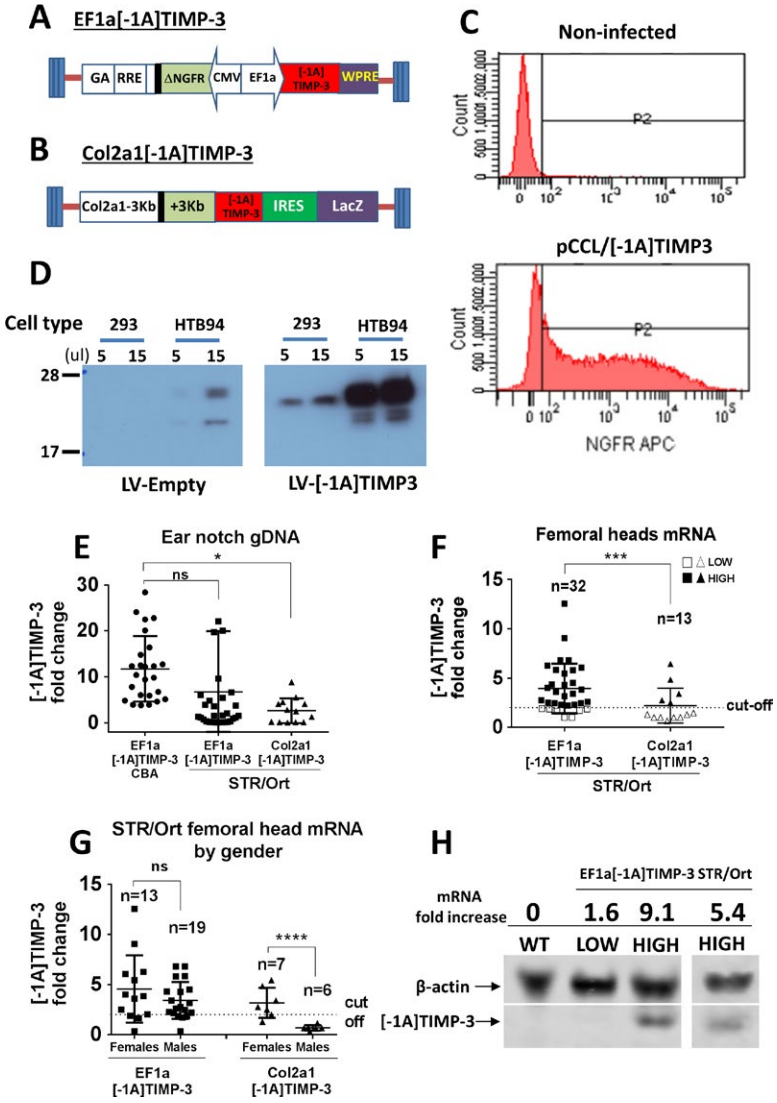

Figure 1. Evaluation of lentiviral expression. **A** and **B**, Illustrations of constructed vectors for overexpression of the tissue inhibitor of metalloproteinases 3 (TIMP-3) variant [-1A]TIMP-3 with lentivirus (LV)–driven elongation factor 1α (EF-1α) promoter (**A**) and conditional Col2a1-driven transductions (**B**) are shown. **C**, Chondrocytic HTB94 cells, analyzed by flow cytometry, show increased expression of nerve growth factor receptor (NGFR) in cells expressing the lentiviral transgene. APC = allophycocyanin. **D**, Western blots of HTB94 cells show small quantities of endogenous TIMP-3 in lentiviral empty vector (LV-empty) compared with high protein levels in both HEK 293 and HTB94 [-1A]TIMP-3–overexpressing cells (LV-[-1A]TIMP-3). **E**, Integration of [-1A]TIMP-3 into genomic DNA (gDNA) extracted from ear notches in all mice was evaluated by quantitative polymerase chain reaction. STR/Ort mice in the Col2a1[-1A]TIMP-3–transgenic group expressed significantly lower levels of [-1A]TIMP-3 compared with EF-1α[-1A]TIMP-3–transgenic CBA control mice. NS = not significant. **F**, Quantification of [-1A]TIMP-3 mRNA in femoral heads of STR/Ort mice showed higher expression in EF-1α[-1A]TIMP-3–transgenic mice. Mice were separated according to high and low levels of [-1A]TIMP-3 mRNA expression, with a cutoff value of 2-fold difference. **G**, Males expressed lower levels of [-1A]TIMP-3 than did females in both transgenic groups, and the difference was significant in Col2a1[-1A]TIMP-3–transgenic mice. **H**, Western blot confirmed increasing levels of [-1A]TIMP-3 protein in STR/Ort mice expressing higher amounts of [-1A]TIMP-3 mRNA compared with STR/Ort mice expressing lower amounts of [-1A]TIMP-3 mRNA and compared with wild-type (WT) mice. In **E–G**, symbols represent individual mice; bars show the mean ± SD. * = $P < 0.05$; *** = $P < 0.001$; **** = $P < 0.0001$.

goat anti-rabbit secondary antibodies (IRDye 680RD for actin and 800CW for TIMP-3; Li-Cor), and relative quantitation was conducted with β-actin as a reference protein.

Quantitative PCR. Integration of [-1A]TIMP-3 cDNA and overexpression were monitored by qPCR at both genomic DNA and messenger RNA (mRNA) levels (for details, see Supplementary Methods, http://onlinelibrary.wiley.com/doi/10.1002/art.40765/abstract).

Micro–computed tomography (micro-CT). Left and right hind limbs of all STR/Ort mice were dissected and immediately

scanned using a Skyscan 1272 micro-CT scanner (Bruker) at 50 kV, 0.5 aluminum filter, 200 mA, voxel size 9.00 μm, and 0.3° rotation angle. Data sets were reconstructed using NRecon reconstruction software, and 3-dimensional volumes of interest were selected using Dataviewer and CTAn software. Morphometric parameters were analyzed for tibial metaphyseal trabecular bone, cortical bone in diaphysis, and subchondral bone in epiphysis as previously described (33,34) (for details, see Supplementary Methods, http://onlinelibrary.wiley.com/doi/10.1002/art.40765/abstract).

In vitro bone cell culture and mineralization assay. STR/Ort and CBA mouse–derived primary osteoblasts were isolated, and their mineralization capacity was assessed by alizarin red S staining after 4 weeks. To assess the in vitro osteoregulatory effect of [-1A]TIMP-3, osteoblasts were isolated from skeletally mature 12-week-old wild-type (WT) C57BL/6 mice and infected with [-1A]TIMP-3 or TIMP-3 lentiviruses, while untreated and lentivirus–mock-infected osteoblasts served as controls. Early mineralization capacity of the infected osteoblasts was evaluated with alizarin red S staining after 21 days (for details, see Supplementary Methods, http://onlinelibrary.wiley.com/doi/10.1002/art.40765/abstract).

Histologic evaluation of cartilage lesions in STR/Ort mice. Following micro-CT, knee joints from all STR/Ort mice were fixed in 4% paraformaldehyde solution for 24 hours, decalcified in 10% EDTA for 3 weeks, and subsequently stored in 70% ethanol until processing. Samples were embedded in paraffin wax and sectioned coronally (5 μm thickness) through the entire joint. Proteoglycan loss was evaluated using Safranin O–fast green staining and a validated scoring system following the Osteoarthritis Research Society International (OARSI) recommendations (35). Joints were scored in a blinded manner by 2 experienced investigators (IK and BP), and scores were averaged using a modification to the methods of Poulet et al (18). To obtain robust results, as OA affects predominantly the medial tibial plateau and medial femoral condyle, the average of the maximum scores at both sites was used for each sample. Mean scores were calculated as the average of the scores recorded at 8 levels at 90-μm intervals across the entire joint.

Immunohistochemistry. For immunohistochemistry experiments, sections were deparaffinized, rehydrated, and probed with selected antibodies. Two percent normal goat serum was used for blocking. For [-1A]TIMP-3 detection, an additional step of antigen retrieval was applied by incubation with chondroitinase ABC (Sigma) at 0.01 units/ml. Rabbit anti-mouse TIMP-3 polyclonal antibody against the C-terminus of TIMP-3 (Millipore) was used at 1:3,000 dilution in normal goat serum. Rabbit anti-mouse anti-NVTEGE antibody (1:850), kindly provided by Dr. J. S. Mort (36), was used for detection of ADAMTS-generated neoepitopes. Nonimmune rabbit serum was used as negative control. Primary antibodies were detected using a Vectastain ABC kit with a secondary goat anti-rabbit biotinylated antibody (Vector) and visualized with HRP-conjugated streptavidin using 3,3′-diaminobenzidine.

Statistical analysis. All data were analyzed with GraphPad Prism 6 software and expressed as the mean ± SD. Data sets were tested for Gaussian distribution with the D'Agostino-Pearson normality test. Comparisons between ≥3 groups were performed by one-way analysis of variance followed by Tukey's multiple comparisons post hoc test. The Mann-Whitney U test or Student's 2-tailed *t*-test was used to compare 2 groups. Correlations were performed with Pearson's test. In all cases, *P* values less than 0.05 were considered significant.

RESULTS

In vitro efficacy of [-1A]TIMP-3 lentiviral transduction. In order to evaluate efficacy of lentiviral transduction, we infected the human embryonic kidney cell line (HEK 293) as well as the chondrosarcoma HTB94 cell line with a lentiviral construct (Figure 1A). Approximately 75% of HTB94 cells transduced with the [-1A]TIMP-3–containing vector expressed the NGFR marker, which is coexpressed by the same vector; in contrast, there was no detectible NGFR marker expression in uninfected control HTB94 cells (Figure 1C).

Western blot analysis showed that control HTB94 cells transduced by empty lentiviral vector secreted a small amount of endogenous TIMP-3 protein into the medium, detected by the anti–TIMP-3 antibody. In contrast, a high level of [-1A]TIMP-3 protein was secreted by HTB94 cells infected with EF-1α[-1A]TIMP-3 lentivirus compared with a lower level of protein from HEK 293 cells (Figure 1D). The data demonstrate effective lentivirus transduction into different types of cells and overexpression of the [-1A]TIMP-3 transgene in chondrocytes.

Transgenic overexpression of [-1A]TIMP-3 in mice. We generated several transgenic lines using 2 different methods. Lentivirus-induced global [-1A]TIMP-3–transgenic mice (EF-1α[-1A]TIMP-3–transgenic mice) were compared with conditional Col2a1[-1A]TIMP-3–transgenic mice. The method of pronuclear injection of fertilized STR/Ort mouse eggs using Col2a1[-1A]TIMP-3 linearized plasmid resulted in a low level of integration of the transgene, as determined by qPCR of genomic DNA from ear notches (Figure 1E). In order to determine mRNA expression levels within STR/Ort transgenic mice, total RNA was extracted from whole mouse femoral heads. Quantitative PCR using a specific primer for FLAG tag at the 3′-end of [-1A]TIMP-3 to distinguish endogenous from transgenic mRNA resulted in a range of mRNA overexpression, ranging between a ≤2-fold and a 13-fold increase (Figure 1F).

Most mice expressing high levels of [-1A]TIMP-3 mRNA were generated from lentiviral infection. [-1A]TIMP-3 mRNA levels were consistent across paired left and right femoral heads in both EF-1α[-1A]TIMP-3– and Col2a1[-1A]TIMP-3–transgenic groups of mice, but lower levels of expression were noted in males compared with females, especially in those of the Col2a1[-1A]TIMP-3–transgenic group, perhaps because of smaller group size (Figure 1G). Western blot showed undetectable [-1A]TIMP-3 protein levels in WT and low expressers but 5–10-fold greater levels in mice deemed high expressers based on an assessment of their [-1A]TIMP-3 mRNA levels (Figure 1H).

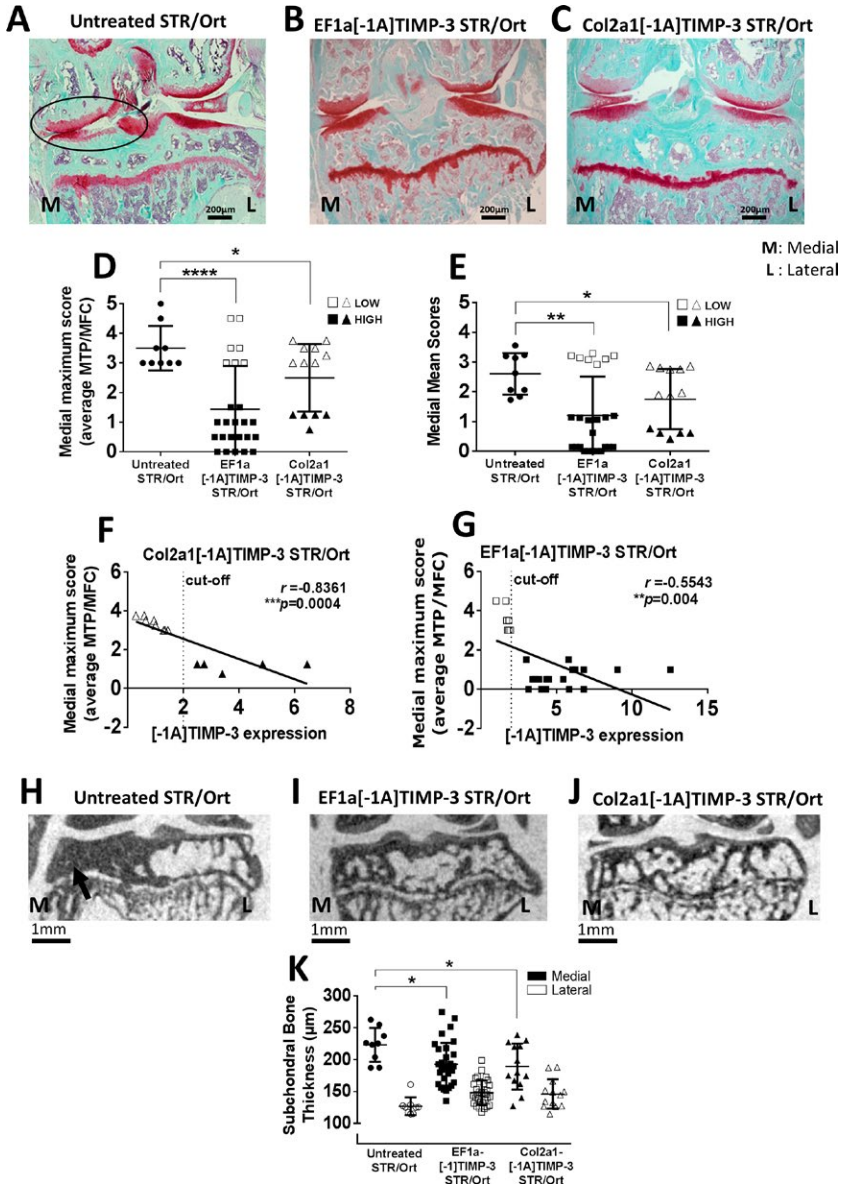

Figure 2. Overexpression of [-1A]TIMP-3 protects against osteoarthritis (OA) cartilage degradation in STR/Ort mice. **A–C**, Untreated STR/Ort mice at age 40 weeks show severe OA erosion in the medial sites of the tibial plateau and femoral condyles (circled in **A**), while both EF-1α[-1A]TIMP-3–transgenic mice (**B**) and Col2a1[-1A]TIMP-3–transgenic mice (**C**) show cartilage protection. **D** and **E**, OA scores of both EF-1α[-1A]TIMP-3–transgenic mice and Col2a1[-1A]TIMP-3–transgenic mice were significantly lower than those of age-matched untreated STR/Ort mice, which had high maximum (**D**) and mean (**E**) OA scores of the knee joints. MTP = medial tibial plateau; MFC = medial femoral condyle. **F** and **G**, Significant negative correlations between [-1A]TIMP-3 expression levels and OA scores were found in Col2a1[-1A]TIMP-3–transgenic mice (**F**) and EF-1α[-1A]TIMP-3–transgenic mice (**G**), which suggests that mice expressing high levels of [-1A]TIMP-3 (solid symbols) were better protected than those expressing low levels of [-1A]TIMP-3 (open symbols). **H–J**, Subchondral bone thickness was assessed by micro–computed tomography, which demonstrated that untreated STR/Ort mice with OA had severe sclerotic lesions (**arrow**) at the medial side of the tibial epiphysis (**H**) compared with EF-1α[-1A]TIMP-3–transgenic mice (**I**) and Col2a1[-1A]TIMP-3–transgenic mice (**J**). **K**, Quantification of subchondral bone thickness showed significant reduction on the medial site, while the lateral site seemed unaffected. In **D**, **E**, and **K**, symbols represent individual mice; bars show the mean ± SD. * = $P < 0.05$; ** = $P < 0.01$; **** = $P < 0.0001$. See Figure 1 for other definitions and explanation of cutoff.

Overall, STR/Ort background transgenic mice were harder to generate by direct pronuclear injection as fewer eggs were fertilized compared with CBA control mice and significant numbers of injected eggs did not survive. Importantly, the various levels of transgene expression achieved allowed us to determine the "threshold" expression level of [-1A]TIMP-3 needed for effective amelioration of the STR/Ort phenotype.

[-1A]TIMP-3 protects against OA cartilage degradation in STR/Ort mice. The main OA features in the STR/Ort mouse knee are cartilage loss on the medial tibial plateau and medial femoral condyle accompanied by osteophyte development and subchondral bone sclerosis (23). Therefore, we investigated these regions in mice age 40 weeks using OARSI maximum and mean OA scores (Figures 2A–E).

We found that while knees of untreated STR/Ort mice at age 40 weeks had severe loss of articular cartilage at the medial tibial plateau and medial femoral condyle (Figure 2A), STR/Ort transgenic mice overexpressing [-1A]TIMP-3 with either EF-1α[-1A]TIMP-3 or Col2a1[-1A]TIMP-3 maintained their articular cartilage (Figures 2B and C). The overall analysis showed a significant reduction or prevention of articular cartilage degradation with a decrease of 57% (mean maximum score 1.4; $P < 0.0001$) for the EF-1α[-1A]TIMP-3–transgenic group and a decrease of 22% (mean maximum score 2.5; $P = 0.0165$) for the Col2a1[-1A]TIMP-3–transgenic group, compared with untreated STR/Ort mice (mean maximum score 3.2) (Figure 2D). Similarly, mean scores at the medial sites for both overexpressing STR/Ort groups were significantly lower than those in the untreated group ($P = 0.005$ for the EF-1α[-1A]TIMP-3–transgenic group and $P = 0.043$ for the Col2a1[-1A]TIMP-3–transgenic group) (Figure 2E). Furthermore, there was a negative correlation between maximum OA score and [-1A]TIMP-3 expression levels, indicating a protective effect of [-1A]TIMP-3 when it is expressed at high levels (Figures 2F and G). A careful examination of stained sections revealed that mice expressing high levels of [-1A]TIMP-3 also showed signs of reduced proteoglycan accumulation in the cruciate ligaments, restored medial collateral ligament physiology, ameliorated osteophyte formation, and abolished synovial activation and inflammatory cell infiltration, which are known hallmarks of OA in this strain (see Supplementary Figure 1, http://onlinelibrary.wiley.com/doi/10.1002/art.40765/abstract).

The micro-CT data showed that untreated STR/Ort controls had severe subchondral sclerosis on the medial side of the knee joint (Figures 2H and K). This subchondral bone thickening was abrogated both in EF-1α[-1A]TIMP-3–transgenic STR/Ort mice and in Col2a1[-1A]TIMP-3–transgenic STR/Ort mice (Figures 2I–K).

Localization of [-1A]TIMP-3 and inhibition of aggrecanases in rescued cartilage. To validate whether the reduction in articular cartilage degradation and diminished aggrecanase cleavage is linked directly to overexpression of [-1A]TIMP-3, immunohistologic labeling for [-1A]TIMP-3 and the aggrecan NVTEGE neoepitope was done on adjacent knee joint sections. Figure 3A shows a representative coronal section of protected knee joint from STR/Ort mice in which [-1A]TIMP-3 immunostaining was seen in the adjacent section; [-1A]TIMP-3 was evident in both menisci and articular cartilage (Figure 3B) and resembled the endogenous TIMP-3 localization with pericellular distribution, as previously described (37).

Immunostaining against the NVTEGE neoepitope, an ADAMTS catabolic product, revealed that the medial side of the joints in OA-prone STR/Ort mice expressing low levels of the transgene (Figure 3F) showed little if any labeling for the NVTEGE neoepitope due to the extensive cartilage damage (verified by Safranin O staining) (Figure 3D) and the likely loss of known matrix binding partners for this antigen. This was consistent with NVTEGE-positive labeling (Figure 3F) in the apparently intact sites directly neighboring this damaged OA cartilage tissue, into which OA development was likely actively advancing. The lateral compartment, which is OA-resistant even in the STR/Ort strain, retained relatively intact cartilage compared with the medial side, yet already exhibited slight proteoglycan loss (evidenced by Safranin O staining) (Figure 3E) that colocalized with NVTEGE-positive labeling (Figure 3G). In contrast, STR/Ort mice expressing high levels of the transgene, which exhibited protection against OA and therefore retention of intact cartilage in both medial (Figure 3I) and lateral (Figure 3J) knee joint compartments, did not show NVTEGE-positive labeling (Figures K–M). This was consistent with [-1A]TIMP-3–related inhibition of ADAMTS-mediated aggrecan degradation.

Selective inhibition of aggrecanases increases bone mass in vivo. Given that STR/Ort mice, especially female mice (22), show increased trabecular bone mass, we examined bone mass (expressed as percentage trabecular bone volume/total tissue volume [%BV/TV]) using micro-CT in the tibial metaphysis of all mice overexpressing the transgene in comparison with untreated STR/Ort mice and EF-1α[-1A]TIMP-3–transgenic CBA control mice. Consistent with previous findings, nontransgenic untreated STR/Ort mice showed significantly increased BV/TV compared with CBA mice (22). Intriguingly, tibial BV/TV was further increased both in EF-1α[-1A]TIMP-3–transgenic mice and in Col2a1[-1A]TIMP-3–transgenic mice compared with untreated STR/Ort mice (Figure 4A) (representative images are shown in Figure 4E), and this was consistent with the other micro-CT trabecular bone parameters (see Supplementary Table 3, http://onlinelibrary.wiley.com/doi/10.1002/art.40765/abstract). The extent of this elevation in BV/TV was greater in EF-1α[-1A]TIMP-3–transgenic mice, presumably due to higher levels of [-1A]TIMP-3 mRNA overexpression. Subgroup analysis of mice expressing low and high levels of [-1A]TIMP-3 showed a statistically significant increase in BV/TV only in STR/Ort mice express-

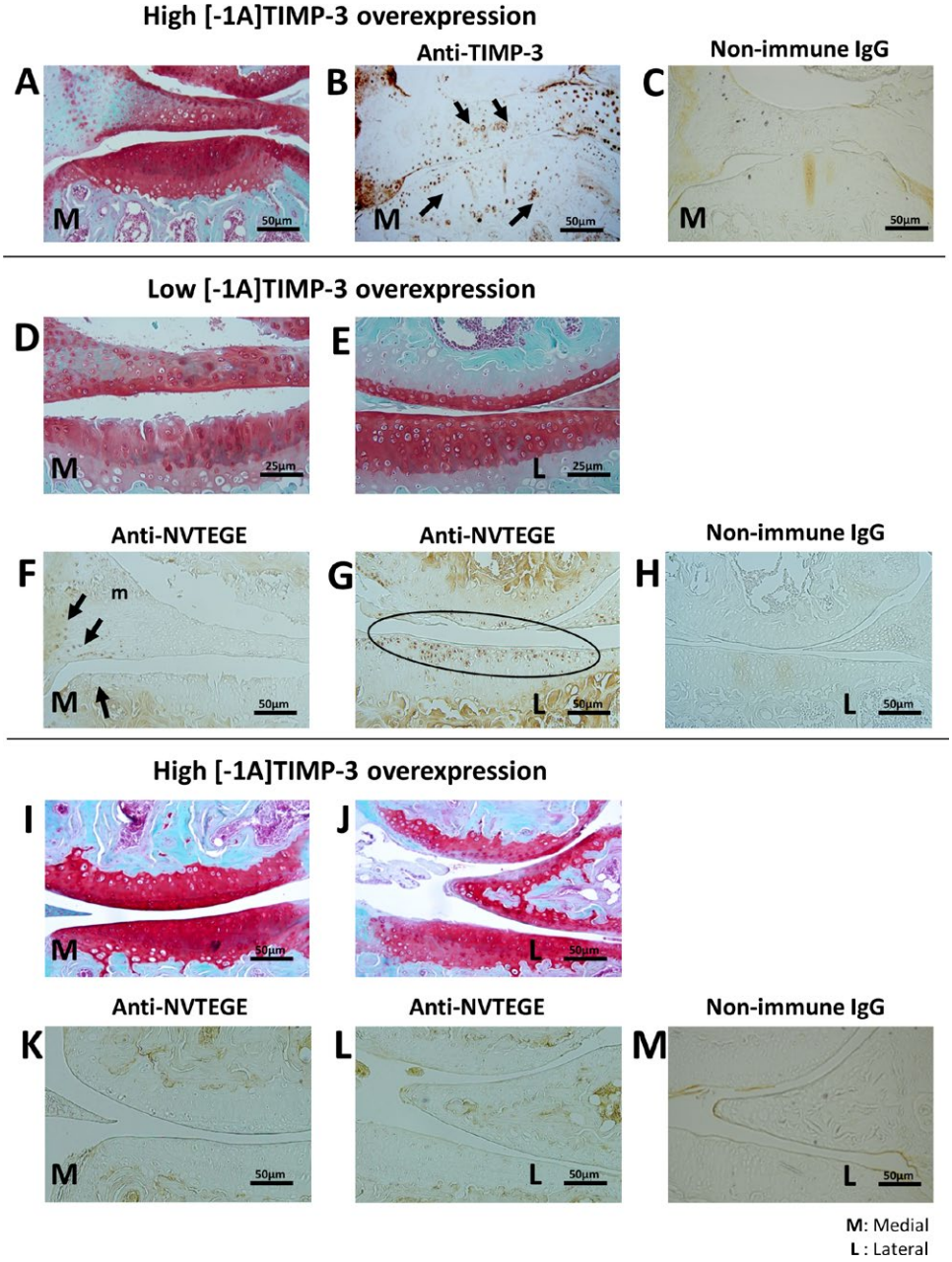

Figure 3. Localization of the tissue inhibitor of metalloproteinases 3 (TIMP-3) variant [-1A]TIMP-3 and inhibition of aggrecanase activity in articular cartilage. **A–C**, Mice expressing high levels of [-1A]TIMP-3, which were protected against osteoarthritis as revealed by Safranin O staining (**A**), showed immunohistochemical staining for anti–TIMP-3 antibody (**arrows** in **B**), which indicated that [-1A]TIMP-3 protein was translated at high levels. Rabbit IgG was used as negative control (**C**). **D** and **F**, STR/Ort mice expressing low levels of the transgene showed cartilage degradation at the medial site (**D**), which was concomitant with a lack of ADAMTS-derived NVTEGE neoepitope in the adjacent section (**F**), where **arrows** indicate peripheral neoepitope staining in meniscus (**m**) and cartilage matrix not yet affected by proteolysis (**F**). **E, G**, and **H**, Safranin O staining of the lateral condyle and plateau shows slight proteoglycan loss (**E**) colocalizing with NVTEGE-positive labeling (circled in **G**). Rabbit IgG was used as negative control (**H**). **I–M**, In contrast, in mice expressing high levels of [-1A]TIMP-3, cartilage matrix integrity was maintained at both medial (**I**) and lateral (**J**) sites, with undetectable levels of NVTEGE at either site (**K** and **L**), which suggests that ADAMTS-4/5 neoepitopes were inhibited by [-1A]TIMP-3. Rabbit IgG was used as negative control (**M**).

ing high levels of [-1A]TIMP-3 (Figure 4B). A similar trend was observed in EF-1α[-1A]TIMP-3–transgenic CBA control mice (Figure 4C).

Data subanalysis based on separation by sex revealed that STR/Ort females of both transgenic mouse lines had substantially higher bone mass than untreated controls (Figure 4D). The difference was greater in female EF-1α[-1A]TIMP-3–transgenic mice expressing high levels of [-1A]TIMP-3. Male STR/Ort mice, which expressed relatively lower overall levels of [-1A]TIMP-3, similarly showed higher bone mass in the EF-1α[-1A]TIMP-3–

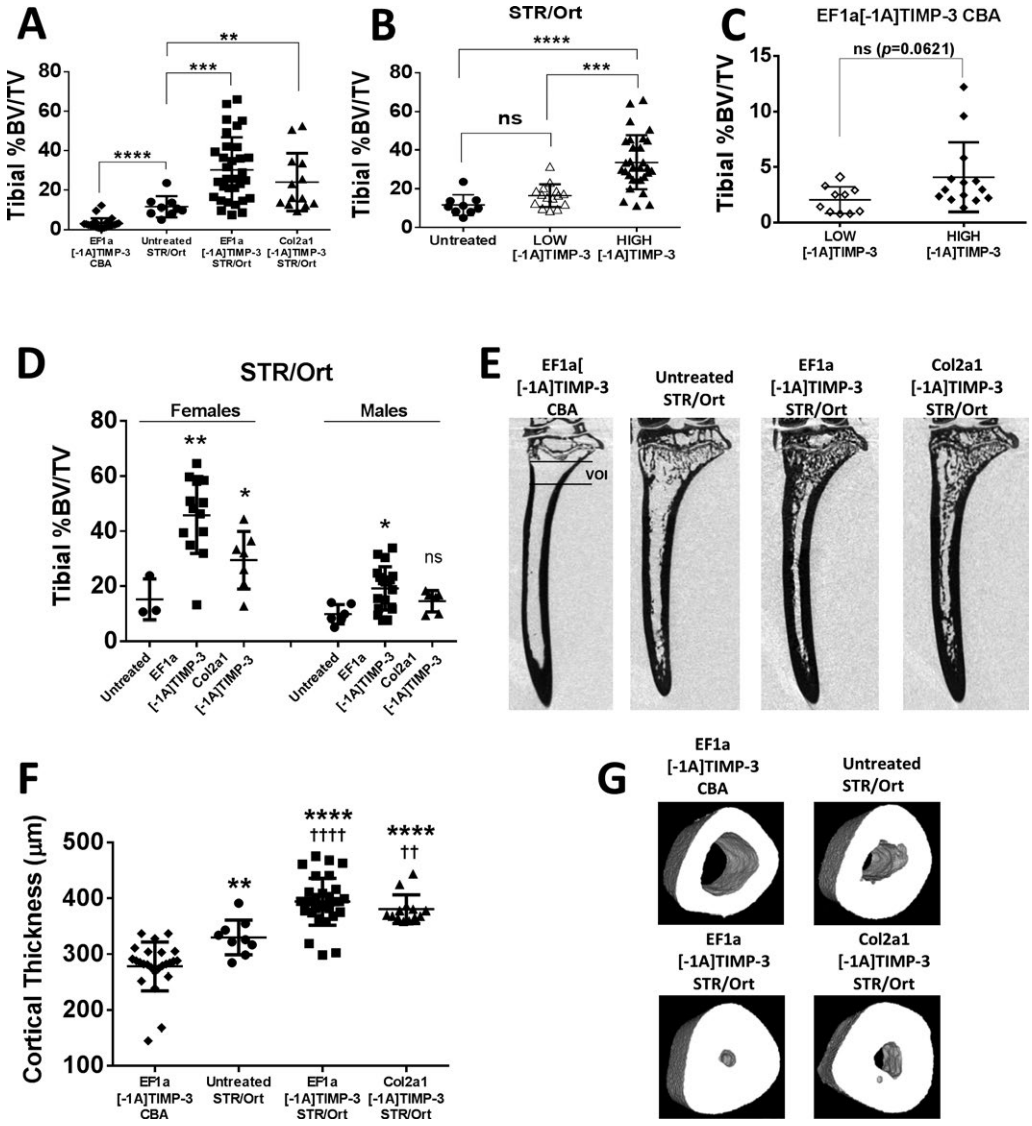

Figure 4. Selective inhibition of aggrecanases by [-1A]TIMP-3 leads to augmented bone mass in vivo. **A**, Micro–computed tomography trabecular analysis showed that untreated STR/Ort mice have significantly increased bone mass compared with EF-1α[-1A]TIMP-3–transgenic CBA mice. EF-1α[-1A]TIMP-3–transgenic mice and Col2a1[-1A]TIMP-3–transgenic mice both had significantly increased bone mass compared with untreated STR/Ort mice. **B**, Elevation of bone volume/total tissue volume (BV/TV) was observed only in STR/Ort mice expressing high levels of [-1A]TIMP-3 (solid symbols), while BV/TV in STR/Ort mice expressing low levels of [-1A]TIMP-3 (open symbols) did not differ from BV/TV in untreated STR/Ort mice. **C**, The increase in BV/TV in EF-1α[-1A]TIMP-3–transgenic CBA mice expressing high levels of [-1A]TIMP-3 was not significant. **D**, Analysis according to sex showed that STR/Ort females overexpressing either transgene had significantly higher bone mass compared with untreated STR/Ort females, while in STR/Ort males an increase in bone mass was observed only in the EF-1α[-1A]TIMP-3–transgenic group. **E**, Representative images from groups of STR/Ort female mice are shown, as well as an image representing a group of female EF-1α[-1A]TIMP-3–transgenic CBA mice. Lines show the bone volume of interest (VOI) that was analyzed in this experiment. **F**, The same results were observed with cortical bone measurements in the same groups of female mice represented in **E**. **G**, Results of cortical bone measurements in **F** are represented visually. In **A–D** and **F**, symbols represent individual mice; bars show the mean ± SD. In **A**–**C**, ** = $P <$ 0.01; *** = $P < 0.001$; **** = $P < 0.0001$. In **D**, * = $P < 0.05$; ** = $P < 0.01$ versus untreated STR/Ort mice. In **F**, ** = $P < 0.01$; **** = $P < 0.0001$ versus EF-1α[-1A]TIMP-3–transgenic CBA mice, and †† = $P < 0.01$; †††† = $P < 0.0001$ versus untreated STR/Ort mice. See Figure 1 for other definitions.

transgenic group compared with untreated STR/Ort mice (Figure 4D). Finally, cortical bone analysis revealed increased mean cortical bone thickness in transgenic STR/Ort mice, demonstrating that the effect of [-1A]TIMP-3 overexpression on bone tissue also extends to cortical bone regions (Figures 4F and G).

[-1A]TIMP-3 enhances in vitro bone formation. The next sets of experiments were devised, first, to determine whether the increase in bone mass is coupled with sustained changes in osteoblasts isolated from CBA and STR/Ort mice with divergent levels of [-1A]TIMP-3 transgene overexpres-

sion, and second, to test whether enhanced bone mass in transgenic mice was related to a developmental program that was abrogated by aggrecanase inhibition, or whether changes in isolated adult osteoblasts correspond to greater bone formation observed in [-1A]TIMP-3–overexpressing mice. Primary osteoblasts were isolated from long bones of CBA and STR/Ort EF-1α[-1A]TIMP-3–overexpressing mice, and the level of mineralization was assessed using alizarin red S staining. Results showed that the level of mineralization in isolated osteoblasts depended on the level of [-1A]TIMP-3 expression (Figures 5A and B); higher [-1A]TIMP-3 expression levels in both STR/Ort and CBA mice were associated with a greater extent of mineralization, with osteoblasts from these mice forming larger and more numerous bone nodules compared

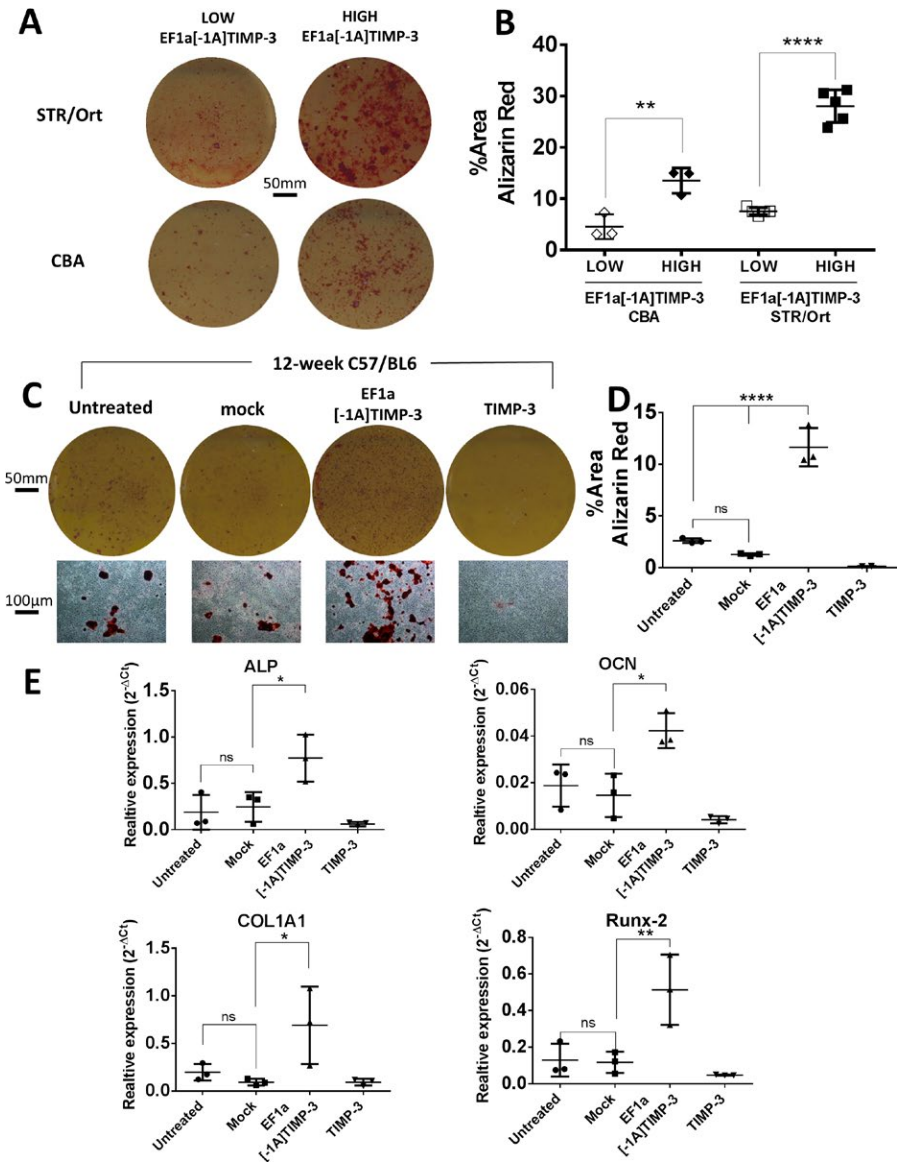

Figure 5. Overexpression of [-1A]TIMP-3 increases bone formation both in transgenic mouse–derived and newly infected primary osteoblasts. **A** and **B**, In vitro bone mineralization assay using alizarin red S staining indicated that long bone osteoblasts derived from EF-1α[-1A]TIMP-3–transgenic STR/Ort and CBA mice expressing high levels of [-1A]TIMP-3 had greater bone-forming capacity than osteoblasts derived from mice in these groups expressing low levels of [-1A]TIMP-3 (**A**), forming more and larger bone nodules with a significantly greater percentage of stained area (**B**) at 28 days of mineralization. **C** and **D**, Mature osteoblasts isolated from 12-week-old C57BL/6 mice were left untreated, mock-infected, or infected with lentiviral [-1A]TIMP-3 or native TIMP-3 and assessed for the extent of mineralization at 21 days (**C**); osteoblasts infected with lentiviral [-1A]TIMP-3 showed a significantly greater rate of mineralization compared with untreated or mock-infected osteoblasts (**D**). **C–E**, In contrast, overexpression of native TIMP-3 completely stopped mineralization of bone matrix. **E**, Osteoblasts infected with lentiviral [-1A]TIMP-3 also showed significantly increased expression of osteogenic gene markers such as alkaline phosphatase (AP), osteocalcin (OC), type I collagen (COL1A1), and the transcription factor Runx-2 compared with untreated or mock-infected osteoblasts. In **B**, **D**, and **E**, symbols represent individual mice; bars show the mean ± SD. * = $P < 0.05$; ** = $P < 0.01$; **** = $P < 0.0001$. See Figure 1 for other definitions.

with osteoblasts derived from mice expressing low levels of [-1A]TIMP-3.

To further determine whether [-1A]TIMP-3 directly affects osteoblastic bone formation and mineralization in cells that were not previously exposed to the [-1A]TIMP-3 transgene in vivo, we performed in vitro transduction of adult osteoblasts isolated from the long bones of 3-month-old WT mice. We found that [-1A]TIMP-3–transduced osteoblasts formed a significantly increased number of mineralized bone nodules compared with untreated or mock-infected cells (Figures 5C and D). In order to verify that [-1A]TIMP-3 exerts different effects compared with native, endogenous TIMP-3, we extended the experiments to include native TIMP-3. In contrast to transduction with [-1A]TIMP-3, native TIMP-3 completely abrogated bone formation, consistent with our previous in vivo findings, in which overexpression of Col2a1-driven TIMP-3 resulted in significant reduction in bone mass (28). Similarly, expression of mRNA for alkaline phosphatase, osteocalcin, type I collagen, and RUNX-2, reflecting osteogenic stimulation, was found to be elevated in [-1A]TIMP-3–transduced osteoblasts and suppressed by TIMP-3 (Figure 5E).

DISCUSSION

The primary aim of our study was to evaluate whether OA that arises spontaneously in STR/Ort mice can be ameliorated by an aggrecanase inhibitor. We used [-1A]TIMP-3, a modified TIMP-3 that was shown to be a "selective" but not a "specific" inhibitor against aggrecanases in vitro (30).

We compared knee joints of untreated STR/Ort mice with STR/Ort mice that were genetically modified to overexpress [-1A]TIMP-3 either specifically in chondrocytes using the Col2a1 promoter/enhancer Col2a1[-1A]TIMP-3 or ubiquitously through lentiviral transduction using EF-1α[-1A]TIMP-3. The results clearly showed that mice overexpressing [-1A]TIMP-3 had protected articular cartilage or reduced severity of cartilage degradation compared with age-matched, untreated STR/Ort control mice. This protection was dependent on expression levels of [-1A]TIMP-3. Maximum and mean OA scores were lower in mice expressing high levels of [-1A]TIMP-3 and higher in mice expressing low levels of [-1A]TIMP-3, irrespective of lentiviral or Col2a1-selective delivery. Our findings demonstrate the critical roles of aggrecanases in OA pathophysiology in STR/Ort mice, and they highlight that [-1A]TIMP-3 can restrict cartilage aggrecan degradation by blocking aggrecanase activity, and not only that of ADAMTS-4 and ADAMTS-5.

Furthermore, our findings indicate that the characteristic subchondral bone sclerosis observed in the medial site of epiphysis (19,38) was also significantly reduced in response to [-1A]TIMP-3 overexpression. This suggests that [-1A]TIMP-3 may regulate communication between chondrocytes and bone cells, or may indeed have a direct effect on bone through chondrocyte transdifferentiation into osteoblasts (39). Alternatively, we need to explore the possibility that the primary effect of [-1A]TIMP-3 could be the reduction in subchondral bone sclerosis, which in turn improves cartilage stability.

It should be noted that catabolic enzymes such as ADAMTS-4 and ADAMTS-5 are endocytosed by chondrocytes via LRP-1 (25,40) which potentially provides protection for cartilage. It is also notable that LRP-1–mediated endocytic clearance of TIMP-3 (37,41) and [-1A]TIMP-3 is likely to be regulated by LRP-1 (42). This was evident when sulfated glycans (37) inhibited binding of TIMP-3 to LRP-1 or when mutants of LRP-1 binding inhibited metalloproteinase-mediated degradation of cartilage at lower concentrations and for longer periods of time than WT TIMP-3, indicating that their increased half-lives improved their ability to protect cartilage (42).

The fact that the endogenous level of TIMP-3 could be very tightly regulated by LRP-1 at steady state requires an overexpression system rather than knockout to investigate the role of TIMP-3 in vivo, as in the present study in which a significant amount of [-1A]TIMP-3 protein in mice expressing high levels of the transgene was evident by Western blot, compared with endogenous (WT) TIMP-3. This indicates that the overexpression system overcomes LRP-1–mediated endocytic clearance. However, in OA cartilage and under inflammatory conditions this clearance system is impaired due to increased shedding of LRP-1 (26). It is plausible that LRP-1 shedding, defective LRP-1 clearance, or the apparent role of glucose transporter 4/LRP-1 interaction (14) may be important contributors to the many defects that increase the chances of OA development in STR/Ort mice, but we have not investigated this process. Nonetheless, the selective aggrecanase inhibitor [-1A]TIMP-3 is able to ameliorate the cartilage pathology of these mice.

Another major and surprising finding is related to the effect of [-1A]TIMP-3–mediated aggrecanase inhibition on bone mass. STR/Ort mice have an inherent high bone mass phenotype, which is linked to increased osteoblast numbers and bone formation and reduced osteoclast activity (22). Moreover, STR/Ort females exhibit higher bone mass than males, underlying the reported sexual dimorphism in this strain (19,43). Evidence presented herein shows that STR/Ort mice expressing high levels of [-1A]TIMP-3, especially females, had significantly increased trabecular parameters and cortical bone thickness, compared with control mice and mice expressing low levels of [-1A]TIMP-3. We expected the opposite effect, since our previous studies demonstrated that high levels of WT TIMP-3 overexpression in mouse cartilage led to lack of secondary ossification, and mice with intermediate levels of TIMP-3 had reduced bone mass (28). It has already been shown that MMP deficiency (e.g., deficiencies of MMP-9 and membrane type 1 MMP) can lead to developmental skeletal abnormalities (44,45). The increased bone mass in STR/Ort mice was mirrored in CBA control mice, which suggests that bone augmentation by [-1A]TIMP-3 is not specific to the STR/Ort strain. Taken together, the data suggest that there might be a unique involvement of

aggrecanases in bone metabolism, and they highlight that maintaining skeletal homeostasis depends on balanced matrix remodeling by aggrecanases and collagenases.

The findings from in vitro primary osteoblast mineralization assays show that osteoblasts isolated from STR/Ort mice highly overexpressing [-1A]TIMP-3 had a greater bone-forming capacity. This suggests that bone formation is positively influenced by inhibition of aggrecanases, which warrants further investigation. Most important, this observation was not strain-specific, as in vitro infection of WT osteoblasts from young C57BL/6 mice also resulted in enhanced bone mineralization and induction of osteogenic pathways when transduced by lentivirus overexpressing [-1A]TIMP-3 compared with TIMP-3. Our data suggest that [-1A]TIMP-3 may serve as a novel therapeutic agent in osteoporotic bone loss. This notion is supported by findings indicating that conditional overexpression of bone-specific TIMP-1, an MMP-only inhibitor, in osteoblasts leads to low bone turnover only in females (46).

In conclusion, the spontaneous OA that develops over time in STR/Ort mice is driven by aggrecanases, and [-1A]TIMP-3 overexpression can protect against cartilage damage and subchondral bone thickening in this mouse model. In addition, high levels of [-1A]TIMP-3 overexpression also led to a significant increase in bone mass, which highlights a possible dual role of this molecule as a regulator of cartilage and bone homeostasis. In the absence of an effective OA treatment, our novel data show that [-1A]TIMP-3 or other similar molecules exhibiting selective affinity for aggrecanases could be strong candidates for treatment of OA and osteoporosis.

ACKNOWLEDGMENT

The authors are grateful to Professor Hideaki Nagase for providing the cDNA for the [-1A]TIMP-3.

AUTHOR CONTRIBUTIONS

All authors were involved in drafting the article or revising it critically for important intellectual content, and all authors approved the final version to be published. Dr. Bou-Gharios had full access to all of the data in the study and takes responsibility for the integrity of the data and the accuracy of the data analysis.

Study conception and design. Kanakis, Pitsillides, Bou-Gharios.
Acquisition of data. Kanakis, Liu, Javaheri.
Analysis and interpretation of data. Kanakis, Liu, Poulet, Javaheri, van 't Hof.

REFERENCES

1. Neuhold LA, Killar L, Zhao W, Sung ML, Warner L, Kulik J, et al. Postnatal expression in hyaline cartilage of constitutively active human collagenase-3 (MMP-13) induces osteoarthritis in mice. J Clin Invest 2001;107:35–44.
2. Fuchs S, Skwara A, Bloch M, Dankbar B. Differential induction and regulation of matrix metalloproteinases in osteoarthritic tissue and fluid synovial fibroblasts. Osteoarthritis Cartilage 2004;12:409–18.
3. Yang CY, Chanalaris A, Troeberg L. ADAMTS and ADAM metalloproteinases in osteoarthritis—looking beyond the 'usual suspects'. Osteoarthritis Cartilage 2017;25:1000–9.
4. Verma P, Dalal K. ADAMTS-4 and ADAMTS-5: key enzymes in osteoarthritis. J Cell Biochem 2011;112:3507–14.
5. Echtermeyer F, Bertrand J, Dreier R, Meinecke I, Neugebauer K, Fuerst M, et al. Syndecan-4 regulates ADAMTS-5 activation and cartilage breakdown in osteoarthritis. Nat Med 2009;15:1072–6.
6. Glyn-Jones S, Palmer AJ, Agricola R, Price AJ, Vincent TL, Weinans H, et al. Osteoarthritis. Lancet 2015;386:376–87.
7. Nagase H, Kashiwagi M. Aggrecanases and cartilage matrix degradation. Arthritis Res Ther 2003;5:94–103.
8. Nemunaitis J, Poole C, Primrose J, Rosemurgy A, Malfetano J, Brown P, et al. Combined analysis of studies of the effects of the matrix metalloproteinase inhibitor marimastat on serum tumor markers in advanced cancer: selection of a biologically active and tolerable dose for longer-term studies. Clin Cancer Res 1998;4:1101–9.
9. Glasson SS, Askew R, Sheppard B, Carito B, Blanchet T, Ma HL, et al. Deletion of active ADAMTS5 prevents cartilage degradation in a murine model of osteoarthritis. Nature 2005;434:644–8.
10. Stanton H, Rogerson FM, East CJ, Golub SB, Lawlor KE, Meeker CT, et al. ADAMTS5 is the major aggrecanase in mouse cartilage in vivo and in vitro. Nature 2005;434:648–52.
11. Botter SM, Glasson SS, Hopkins B, Clockaerts S, Weinans H, van Leeuwen JP, et al. ADAMTS5-/- mice have less subchondral bone changes after induction of osteoarthritis through surgical instability: implications for a link between cartilage and subchondral bone changes. Osteoarthritis Cartilage 2009;17:636–45.
12. Glasson SS, Askew R, Sheppard B, Carito BA, Blanchet T, Ma HL, et al. Characterization of and osteoarthritis susceptibility in ADAMTS-4–knockout mice. Arthritis Rheum 2004;50:2547–58.
13. Little CB, Mittaz L, Belluoccio D, Rogerson FM, Campbell IK, Meeker CT, et al. ADAMTS-1–knockout mice do not exhibit abnormalities in aggrecan turnover in vitro or in vivo. Arthritis Rheum 2005;52:1461–72.
14. Gorski DJ, Xiao W, Li J, Luo W, Lauer M, Kisiday J, et al. Deletion of ADAMTS5 does not affect aggrecan or versican degradation but promotes glucose uptake and proteoglycan synthesis in murine adipose derived stromal cells. Matrix Biol 2015;47:66–84.
15. Brewster M, Lewis EJ, Wilson KL, Greenham AK, Bottomley KM. Ro 32-3555, an orally active collagenase selective inhibitor, prevents structural damage in the STR/ORT mouse model of osteoarthritis. Arthritis Rheum 1998;41:1639–44.
16. Chiusaroli R, Visentini M, Galimberti C, Casseler C, Mennuni L, Covaceuszach S, et al. Targeting of ADAMTS5's ancillary domain with the recombinant mAb CRB0017 ameliorates disease progression in a spontaneous murine model of osteoarthritis. Osteoarthritis Cartilage 2013;21:1807–10.
17. Mason RM, Chambers MG, Flannelly J, Gaffen JD, Dudhia J, Bayliss MT. The STR/ort mouse and its use as a model of osteoarthritis. Osteoarthritis Cartilage 2001;9:85–91.
18. Poulet B, Ulici V, Stone TC, Pead M, Gburcik V, Constantinou E, et al. Time-series transcriptional profiling yields new perspectives on susceptibility to murine osteoarthritis. Arthritis Rheum 2012;64:3256–66.
19. Staines KA, Poulet B, Wentworth DN, Pitsillides AA. The STR/Ort mouse model of spontaneous osteoarthritis: an update. Osteoarthritis Cartilage 2017;25:802–8.
20. Chambers MG, Cox L, Chong L, Suri N, Cover P, Bayliss MT, et al. Matrix metalloproteinases and aggrecanases cleave aggrecan in different zones of normal cartilage but colocalize in the development of osteoarthritic lesions in STR/Ort mice. Arthritis Rheum 2001;44:1455–65.

21. Flannelly J, Chambers MG, Dudhia J, Hembry RM, Murphy G, Mason RM, et al. Metalloproteinase and tissue inhibitor of metalloproteinase expression in the murine STR/Ort model of osteoarthritis. Osteoarthritis Cartilage 2002;10:722–33.
22. Pasold J, Engelmann R, Keller J, Joost S, Marshall RP, Frerich B, et al. High bone mass in the STR/Ort mouse results from increased bone formation and impaired bone resorption and is associated with extramedullary hematopoiesis. J Bone Miner Metab 2013;31:71–81.
23. Staines KA, Madi K, Mirczuk SM, Parker S, Burleigh A, Poulet B, et al. Endochondral growth defect and deployment of transient chondrocyte behaviors underlie osteoarthritis onset in a natural murine model. Arthritis Rheumatol 2016;68:880–91.
24. Scilabra SD, Yamamoto K, Pigoni M, Sakamoto K, Muller SA, Papadopoulou A, et al. Dissecting the interaction between tissue inhibitor of metalloproteinases-3 (TIMP-3) and low density lipoprotein receptor-related protein-1 (LRP-1): development of a "TRAP" to increase levels of TIMP-3 in the tissue. Matrix Biol 2017;59:69–79.
25. Yamamoto K, Troeberg L, Scilabra SD, Pelosi M, Murphy CL, Strickland DK, et al. LRP-1-mediated endocytosis regulates extracellular activity of ADAMTS-5 in articular cartilage. FASEB J 2013;27:511–21.
26. Yamamoto K, Santamaria S, Botkjaer KA, Dudhia J, Troeberg L, Itoh Y, et al. Inhibition of shedding of low-density lipoprotein receptor–related protein 1 reverses cartilage matrix degradation in osteoarthritis. Arthritis Rheumatol 2017;69:1246–56.
27. Sahebjam S, Khokha R, Mort JS. Increased collagen and aggrecan degradation with age in the joints of Timp3$^{-/-}$ mice. Arthritis Rheum 2007;56:905–9.
28. Poulet B, Liu K, Plumb D, Vo P, Shah M, Staines K, et al. Over-expression of TIMP-3 in chondrocytes produces transient reduction in growth plate length but permanently reduces adult bone quality and quantity. PLoS One 2016;11:e0167971.
29. Javaheri B, Hopkinson M, Poulet B, Pollard AS, Shefelbine SJ, Chang YM, et al. Deficiency and also transgenic overexpression of Timp-3 both lead to compromised bone mass and architecture in vivo. PLoS One 2016;11:e0159657.
30. Wei S, Kashiwagi M, Kota S, Xie Z, Nagase H, Brew K. Reactive site mutations in tissue inhibitor of metalloproteinase-3 disrupt inhibition of matrix metalloproteinases but not tumor necrosis factor-α-converting enzyme. J Biol Chem 2005;280:32877–82.
31. Lim NH, Kashiwagi M, Visse R, Jones J, Enghild JJ, Brew K, et al. Reactive-site mutants of N-TIMP-3 that selectively inhibit ADAMTS-4 and ADAMTS-5: biological and structural implications. Biochem J 2010;431:113–22.
32. Zhou G, Garofalo S, Mukhopadhyay K, Lefebvre V, Smith CN, Eberspaecher H, et al. A 182 bp fragment of the mouse pro α 1(II) collagen gene is sufficient to direct chondrocyte expression in transgenic mice. J Cell Sci 1995;108:3677–84.
33. Van 't Hof RJ. Analysis of bone architecture in rodents using microcomputed tomography. Methods Mol Biol 2012;816:461–76.
34. Huesa C, Ortiz AC, Dunning L, McGavin L, Bennett L, McIntosh K, et al. Proteinase-activated receptor 2 modulates OA-related pain, cartilage and bone pathology. Ann Rheum Dis 2016;75:1989–97.
35. Glasson SS, Chambers MG, Van Den Berg WB, Little CB. The OARSI histopathology initiative: recommendations for histological assessments of osteoarthritis in the mouse. Osteoarthritis Cartilage 2010;18 Suppl 3:S17–23.
36. Mort JS, Roughley PJ. Production of antibodies against degradative neoepitopes in aggrecan. Methods Mol Med 2004;100:237–50.
37. Troeberg L, Lazenbatt C, Anower EK, Freeman C, Federov O, Habuchi H, et al. Sulfated glycosaminoglycans control the extracellular trafficking and the activity of the metalloprotease inhibitor TIMP-3. Chem Biol 2014;21:1300–9.
38. Stok KS, Pelled G, Zilberman Y, Kallai I, Goldhahn J, Gazit D, et al. Revealing the interplay of bone and cartilage in osteoarthritis through multimodal imaging of murine joints. Bone 2009;45:414–22.
39. Javaheri B, Caetano-Silva SP, Kanakis I, Bou-Gharios G, Pitsillides AA. The chondro-osseous continuum: is it possible to unlock the potential assigned within? Front Bioeng Biotechnol 2018;6:28.
40. Yamamoto K, Owen K, Parker AE, Scilabra SD, Dudhia J, Strickland DK, et al. Low density lipoprotein receptor-related protein 1 (LRP1)-mediated endocytic clearance of a disintegrin and metalloproteinase with thrombospondin motifs-4 (ADAMTS-4): functional differences of non-catalytic domains of ADAMTS-4 and ADAMTS-5 in LRP1 binding. J Biol Chem 2014;289:6462–74.
41. Rother S, Samsonov SA, Hempel U, Vogel S, Moeller S, Blaszkiewicz J, et al. Sulfated hyaluronan alters the interaction profile of TIMP-3 with the endocytic receptor LRP-1 clusters II and IV and increases the extracellular TIMP-3 level of human bone marrow stromal cells. Biomacromolecules 2016;17:3252–61.
42. Doherty CM, Visse R, Dinakarpandian D, Strickland DK, Nagase H, Troeberg L. Engineered tissue inhibitor of metalloproteinases-3 variants resistant to endocytosis have prolonged chondroprotective activity. J Biol Chem 2016;291:22160–72.
43. Mahr S, Menard J, Krenn V, Muller B. Sexual dimorphism in the osteoarthritis of STR/Ort mice may be linked to articular cytokines. Ann Rheum Dis 2003;62:1234–7.
44. Engsig MT, Chen QJ, Vu TH, Pedersen AC, Therkidsen B, Lund LR, et al. Matrix metalloproteinase 9 and vascular endothelial growth factor are essential for osteoclast recruitment into developing long bones. J Cell Biol 2000;151:879–89.
45. Holmbeck K, Bianco P, Caterina J, Yamada S, Kromer M, Kuznetsov SA, et al. MT1-MMP-deficient mice develop dwarfism, osteopenia, arthritis, and connective tissue disease due to inadequate collagen turnover. Cell 1999;99:81–92.
46. Geoffroy V, Marty-Morieux C, Le Goupil N, Clement-Lacroix P, Terraz C, Frain M, et al. In vivo inhibition of osteoblastic metalloproteinases leads to increased trabecular bone mass. J Bone Miner Res 2004;19: 811–22.